This document is the Submitted Manuscript version of a Published article that appeared in final form in see International Journal of Pharmaceutics, copyright ELSEVIER.
To access the final edited and published work see: doi: https://doi.org/10.1016/j.ijpharm.2022.121960

Poly(3-hydroxybutyrate): a potential biodegradable excipient for direct 3D printing of pharmaceuticals

Sofia Moroni[1], Shiva Khorshid[1], Annalisa Aluigi[1], Mattia Tiboni[1]*, and Luca Casettari[1]

[1]*Department of Biomolecular Sciences, University of Urbino Carlo Bo, Piazza del Rinascimento, 6, 61029 Urbino (PU), Italy.*

Abstract

During the past decades, 3D printing has revolutionised different areas of research. Despite the considerable progress achieved in 3D printing of pharmaceuticals, the limited choice of suitable materials remains a challenge to overcome. The growing search for sustainable excipients has led to an increasing interest in biopolymers. Poly(3-hydroxybutyrate) (PHB) is a biocompatible and biodegradable biopolymer obtained from bacteria that could be efficiently employed in the pharmaceutical field. Here we aimed to demonstrate its potential application as a thermoplastic material for personalised medicine through 3D printing. More specifically, we processed PHB by using direct powder extrusion, a one-step additive manufacturing technique. To assess and denote the feasibility and versatility of the process, a 3D square model was manufactured in different dimensions (side x height: 12x2 mm; 18x2 mm; 24x2 mm) and loaded with increasing percentages of a model drug (up to 30% w/w). The manufacturing process was influenced by the drug content, and indeed, an increase in the amount of the drug determined a reduction in the printing temperature, without affecting the other parameters (such as the layer height). The composition of the model squares was investigated using Fourier-transform infrared spectroscopy, the resulting spectra confirmed that the starting materials were successfully incorporated into the final formulations. The thermal behaviour of the printed systems was characterized by differential scanning calorimetry, and thermal gravimetric analysis. Moreover, the sustained drug release profile of the formulations was performed over 21 days and showed to be dependent on the dimensions of the printed object and on the amount of loaded drug. Indeed, the formulation with 30% w/w in the dimension 24x2 mm released the highest amount of drug. Hence, the results suggested that PHB and direct powder extrusion technique could be promising tools for the manufacturing of prolonged release and personalised drug delivery forms.

Keywords: Direct Powder Extrusion (DPE); Polyhydroxyalkanoate (PHA); Personalised medicine; Drug delivery; Additive manufacturing

1. Introduction

Three dimensional printing (3DP) is a revolutionary additive manufacturing technology that has been attracting attention in different fields (Ngo et al., 2018). Within the pharmaceutical sector, the applications vary from the direct production of drug delivery systems (*i.e.*, implants, tablets, vaginal rings), to manufacturing and analytical systems (*i.e.*, microfluidic chips) (Tiboni et al., 2021b) (Tiboni et al., 2021a) (Han et al., 2018) (Mathew et al., 2020). Considering the development of dosage forms, owing to the high flexibility, low-cost, and simplicity, 3DP offers unique advantages compared to traditional manufacturing methods. Amongst all, it enables the production of personalised formulations; for instance, in terms of dose, size, and shapes, according to patient's profile (*i.e.*, sex, age, weight, and severity of the disease), and the combination of multiple drugs in a single dose unit. Such patient-centered approach results in improving the acceptability and the adherence to the therapy. In addition, the controlled release profile of the dosage forms is allowed, resulting in the decrease of side effects and the amelioration of compliance (Trenfield et al., 2021) (Seoane-Viaño et al., 2021) (Araújo et al., 2019) (Goyanes et al., 2017). 3DP is a manufacturing tool that use a computer-aided design (CAD) software to create the desired physical object model; subsequently, the model is produced in a layer-by-layer manner after being processed with a computer aided manufacturing (CAM) software. 3DP comprises different techniques, among them, fused deposition modelling (FDM) is the most used in the pharmaceutical field. FDM is based on the employment of a filament made of a thermoplastic material, loaded with the drug of interest. Conventionally, the filament is produced by hot-melt extrusion (HME) before being heated again and extruded to obtain the desired object with the printer. Despite the advantages, including the cost-efficiency, and the wide range of printers and materials available, some drawbacks limit its application. The preparation of the filament, in particular in the case of material mixtures, represents the major difficulty and a further step that divides the CAD design from the final manufacturing. Its optimization is time consuming, and materials are subjected to thermal stress that can affect the stability and lead to possible drug degradation. (Awad et al., 2018) (Melocchi et al., 2020).

A recent alternative to FDM is represented by Direct Powder Extrusion (DPE). DPE enables a single step production process, during which the physical blends of the selected materials, in the form of pellets or powders, are directly processed by a hot melt extruder mounted in the printer. By avoiding the intermediate

step of the filament production and by requiring small amounts of materials, this technique can create an opportunity for local and hospital pharmacies to produce on-demand patient-centered formulations (Fanous et al., 2020). DPE technology has been shown to be a promising and versatile platform for different applications, for instance in the manufacturing of tablets with customized released (Goyanes et al., 2019) (Fanous et al., 2020) (Ong et al., 2020). Moreover, the versatility of the technique also concerns the target of patients to whom it would be compatible. Indeed, it has shown to be suitable for the production of taste-masking tablets for children; proving the applicability of this technique for the development of personalised dosage forms (Boniatti et al., 2021). Nevertheless, the continuous evolution of 3D printing highlights the need to couple the advancements in technology with the research for suitable materials. To tackle this gap, it is important to focus on the material selection.

PHB is a linear homopolyester, that belongs to the family of polyhydroxyalkanoates (PHAs), thermoplastic aliphatic polyesters of biological origin. PHB is mostly obtained from bacterial fermentation as a storage material and accumulated as granules; the degradation occurs through hydrolysis within three to nine months, without exerting negative effects to cells and tissues. Since it is biodegradable, biocompatible and environmental friendly, it can find a variety of applications, including the food packaging industry, tissue engineering, surgical implants, and drug delivery systems, making it a valid alternative to conventional polymers (Elmowafy et al., 2019) (Giubilini et al., 2021) (Koller, 2018) (Martins et al., 2021).

The aim of the present work was to investigate the feasibility of PHB as an alternative excipient for pharmaceutical application through 3DP, specifically with the DPE technique. For this purpose, square geometries were printed in different sizes and loaded with increasing percentages of acetaminophen as model drug. The resulting products were physico-chemically characterized using Fourier-transform infrared spectroscopy (FTIR), differential scanning calorimetry (DSC), thermogravimetric analysis (TGA), and the drug release profiles were determined.

2. Material and Methods

2.1 Materials

Poly(3-hydroxybutyrate), in powder form, was purchased from Biomer (Germany). The key physical features of the polymer are a tensile strength of 15-20 MPa, an elongation of 8-15%, a high crystallinity of 60-70% and a molecular weight >400kDa. Acetaminophen was purchased from A.C.E.F. (Italy). The salts (NaCl, KCl, $Na_2HPO_4*2H_2O$, KH_2PO_4) for preparing the buffer dissolution media were purchased from Merck (Italy). All the solvents used were analytical grade.

2.2 Methods

2.2.1 Preparation of drug-loaded 3D-printed formulation by direct powder extrusion

For each batch, a blend of PHB and acetaminophen was mixed using a powder blender (Atena Galena Top, Atena srl, Italy). Three different percentages of the drug were evaluated (*i.e.*, 10 %, 20 %, and 30 % w/w). The prepared blends (approximately 5 g each) were directly fed into the printing unit consisting of a single-screw powder extruder (3D Cultures, USA) with a nozzle diameter of 1 mm. Before printing, pre-heating took place for approximately 10 minutes. The print speed was set at 20 mm/s; the layer height was 0.6 mm with 100 % of infill density. To avoid the detachment from the plate, a brim was printed as support, in addition, the build plate was kept at 65°C and covered with an adhesion sheet (Polypropylene, Ultimaker, The Netherlands). Printing temperature ranging from 175° to 190°C were used depending on the amount of the drug in the formulations. Printing was performed at room temperature. Three different model square-shape systems were computationally designed (side x height: 12x2 mm, 18x2 mm, and 24x2 mm); files were then converted into print pattern using Ultimaker Cura 4.1 software (Ultimaker, The Netherlands). The printing time per implants were 8/12/16 minutes according to the size. After the printing process, the resulting systems were weighed and measured with a digital calliper (Mitutoyo, Japan) to assess the reproducibility of the printing process.

111 *2.2.2 Characterization of 3D printed geometries*

112 The morphology of the printed square shapes was observed using a Zeiss EVO LS 10 instrument equipped
113 with LaB6 source. Acceleration voltage was 5 kV, and the working distances 4.3 mm or 5.2 mm. Samples
114 were gold-sputtered for 1 min before the analysis.
115 The chemical composition of the printed geometries was compared with the raw materials using attenuated
116 total reflectance Fourier transformed infrared spectroscopy (ATR-FTIR, Spectrum Two FT-IR spectrometer
117 with ATR accessory, Perkin Elmer, MA, USA). Measurements were carried at 450–4000 cm^{-1} with a
118 resolution of 4 cm^{-1} and a total of 64 scans.
119 In addition, differential scanning calorimetry (DSC 6000, Perkin Elmer, USA) and thermogravimetric analysis
120 (TGA 4000, Perkin Elmer, USA) were performed to assess the thermal behaviour of pure acetaminophen, pure
121 PHB, and the formulations after the printing process. For TGA measurements, scans were run from 30 °C to
122 80 °C, at a speed rate of 20 °C/min; subsequently from 80 °C to 500 °C at 10 °C/min; nitrogen was used as
123 purge gas. For DSC analysis, approximately 5 mg samples were placed in aluminium pans and were heated up
124 with a heating rate of 10 °C/min from 30 to 190 °C, hold for 3 min, then cooled down to −30 °C at 30 °C/min,
125 hold for 3 min and finally, heated up again to 190 °C at 10 °C/min. Data collection and analysis were performed
126 using Pyris Manager software (Perkin Elmer, USA).
127

128 *2.2.3 In vitro release study*

129 The release profile of the printed implants was studied in triplicate. For this purpose, each sample was placed
130 into 500 mL of phosphate- buffered saline (PBS) at pH 7.4, under stirring (100 rpm) at 37 °C. For each system,
131 1 mL sample was taken at specified timepoints (1, 2, 3, 7, 10, and 21 days) and replaced with an equal volume
132 of fresh medium. Collected samples were analysed with high-performance liquid chromatography (HPLC,
133 Agilent 1260 Infinity II, Agilent, USA) to quantify the amount of acetaminophen released. For HPLC analysis,
134 a solution of 0.05% trifluoroacetic acid (TFA) in water and acetonitrile were used as mobile phases (ratio
135 85:15), with a flow rate of 1 mL/min in an Agilent Poroshell 120 C18, 100 x 4.6mm, 2.7 μm column (Agilent,
136 USA). The injection volume was 20 μL and the detection was recorded at λ=244 nm (UV lamp), keeping the
137 analysis system at room temperature.

3. Results and discussion

3.1 Morphology

The production of square shape geometries was achieved by directly printing the physical mixtures of the formulations containing the polymer (PHB) and different percentages of the model drug (from 10 % to 30 % w/w). Three different square sizes and different ratios of the model drug were selected to assess the potential application of PHB and direct powder extrusion technique in personalised drug releasing solutions. No significant difference of size between the formulations and the computational object dimensions were evident, suggesting that the printing process reproducibility was ensured. Only the square of 18mm of length x 2 mm of height demonstrated a low variability in the size (up to 1 %). The printed devices are shown in figure 1.

Figure 1. Top view of the printed model systems

The surfaces of the squares were observed using SEM microscope. The SEM images of the printed devices did not show significant differences when increasing the percentage of the model drug. For this reason, figure 2 reports an example of captured images. Observing the top view (Figure 2A), it is possible to visualize the individual layers of the square that are symmetric and that confirmed the acceptable printability of the process. The close-up view shown in figure 2B indicates the presence of a porous structure.

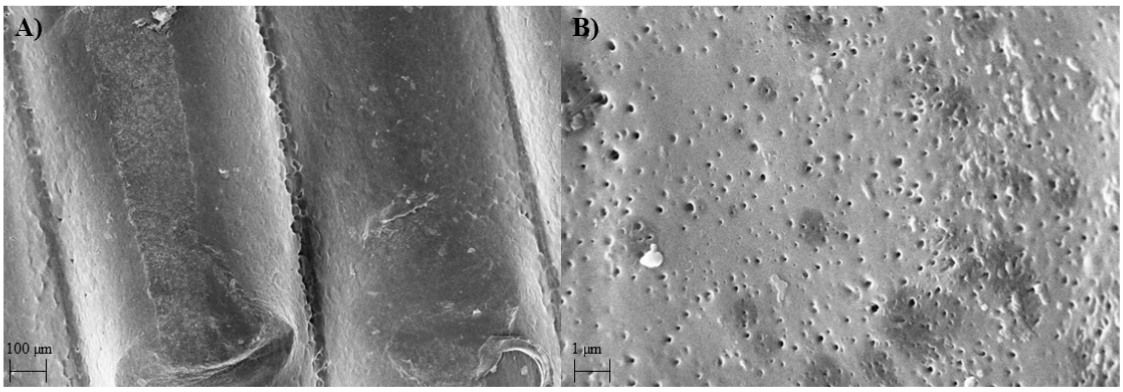

Figure 2. SEM images showing A) the top view of the printed product B) close-up of the top view

3.2 Thermal behaviour

The formulation composition did not affect the printing parameters except for the printing temperature. By increasing the amount of acetaminophen in the formulations, the temperature decreased (as shown in Table 1). This phenomenon can be related to the plasticising effect of the drug on polymers that was already observed in previous studies (Macedo et al., 2020).

Table 1. Printing temperature using DPE.

Sample	***Printing Temperature***
PHB	190 °C
PHB + 10 % A	180 °C
PHB + 20 % A	175 °C
PHB + 30 % A	175 °C

To investigate the effect of acetaminophen on the thermal behaviour of PHB, DSC analysis in the 30-190 °C range was carried out (Figure 3).

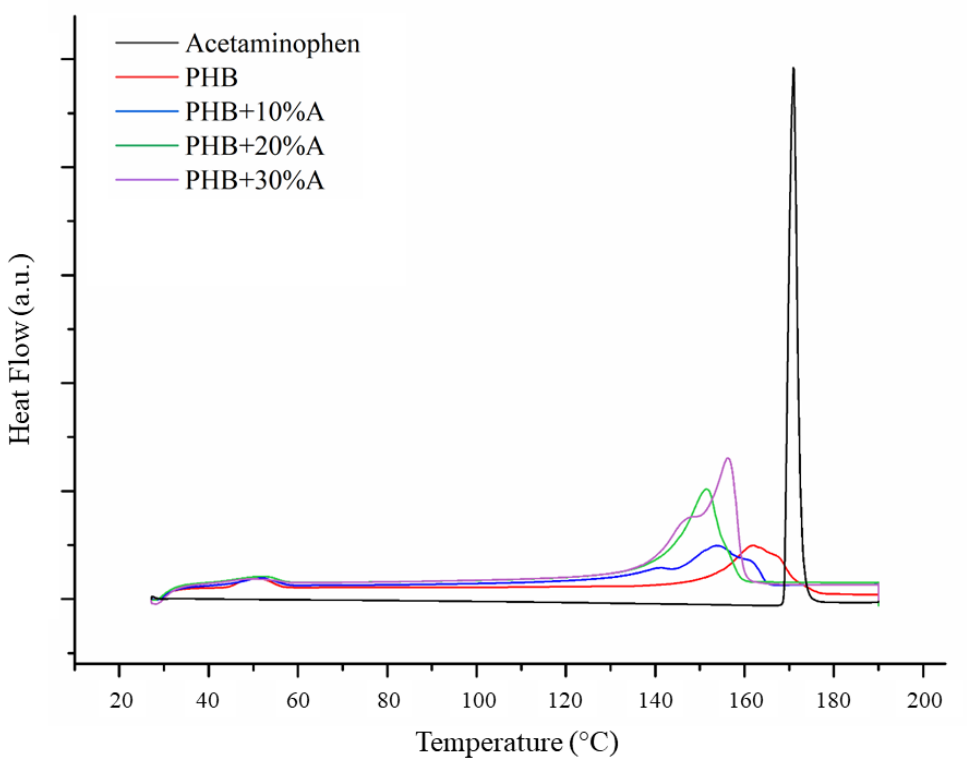

Figure 3. DSC Thermograms of the starting materials and the printed formulations.

As shown, except for acetaminophen, all the thermograms are characterized by a small endothermic peak at about 50 °C related to the evaporation of water adsorbed by the PHB. Moreover, the melting peaks of both pure PHB and acetaminophen loaded samples appear as double melting peaks whose small shoulders are attributed to crystallites with lower size (Gunaratne and Shanks, 2005). In Table 2, the melting temperatures Tm_1 and Tm_2 of the double peaks are reported.

Table 2. Melting temperatures and crystallization degree of the samples.

Sample	**Tm_1 (°C)**	**Tm_2 (°C)**	**χ (%)**	**Tonset (°C)**	**Td (°C)**
PHB	162	168	42	188	296
PHB + 10 % A	154	161	43	189	294
PHB + 20 % A	151	156	59	185	291
PHB + 30 % A	147	156	79	180	283
Acetaminophen	171	#	#	180	283

The addition of acetaminophen up to 20% w/w has a lowering effect on the melting temperatures of the PHB. In particular, the double peak shape undergoes a broadening effect and shift towards lower temperatures, suggesting that the presence of the drug affects the crystallization process of the polymer leading to smaller

crystallites at lower thermal stability. Nevertheless, when the concentration of the acetaminophen increases to 30 % w/w, a double peak was again obtained with the area under the Tm_2 peak is higher than that at Tm_1. It is likely that when 30 % of acetaminophen is added on the PHB, a fraction of the drug lays on the surface without interfering with the crystallization process.

The crystallinity degree (χ) was calculated according to equation 1.

$$\chi(\%) = [\Delta H_m/(\Delta H_{m,0}*\omega_{PHB})]*100 \qquad (1)$$

Where the ΔH_m and $\Delta H_{m,0}$ are the melting enthalpies of the analysed sample and the tabulated 100% crystalline PHB ($\Delta H_{m,0}$=146 J g^{-1}) respectively; while the ω_{PHB} is the weight fraction of PHB in the sample. (Wellen et al., 2015). As reported in Table 2, the crystallinity degree increases with increasing the amount of acetaminophen. According to Sinisi et al. (Sinisi et al., 2021), an increase in crystallinity is consistent with the plasticization effect of the drug since an increase in the molecular mobility could allow the macromolecular chains to rearrange in new configurations resulting in further nucleation. Moreover, the thermogram did not show the endotherm peak of acetaminophen, suggesting that the drug was in the amorphous phase or dissolved in the polymer (Macedo et al., 2020).

The thermal stability of the samples was analysed by TGA (Figure 4A), the onset temperatures (Tonset) and the temperatures corresponding to the maximum degradation rate (Td) were evaluated through DTG (Figure 4B) and are tabulated in Table 2.

The thermal degradation of PHB occurred in two steps: about 88 % of PHB degraded in the main degradation step having a T_{onset} of about 193 °C and a Td at about 296 °C; while a small degradation started at 385 °C with a Td of about 401 °C. A similar degradation trend was observed for the PHB samples loaded with acetaminophen, with the difference being that the weight loss was higher above 280 °C, due to the lower thermal stability of the drug (Figure 4A and B). The T_{onset} and Td temperatures also approaches to those of acetaminophen, as the amount of drug increases (Figure 4B and Table 2).

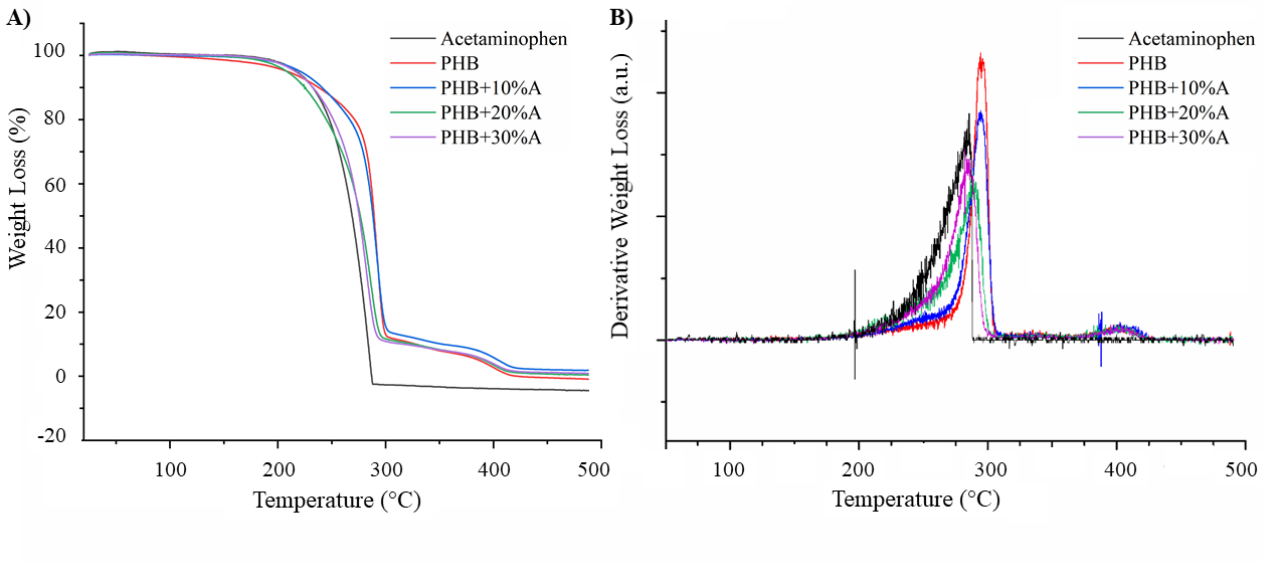

201

202 **Figure 4**. (A) TGA curves and (B) DTGA of printed formulations.

203 *3.3 Molecular and supermolecular characterization*

204 ATR-FTIR was performed to investigate the composition of the printed squares. The resulting spectra are

205 illustrated in figure 5.

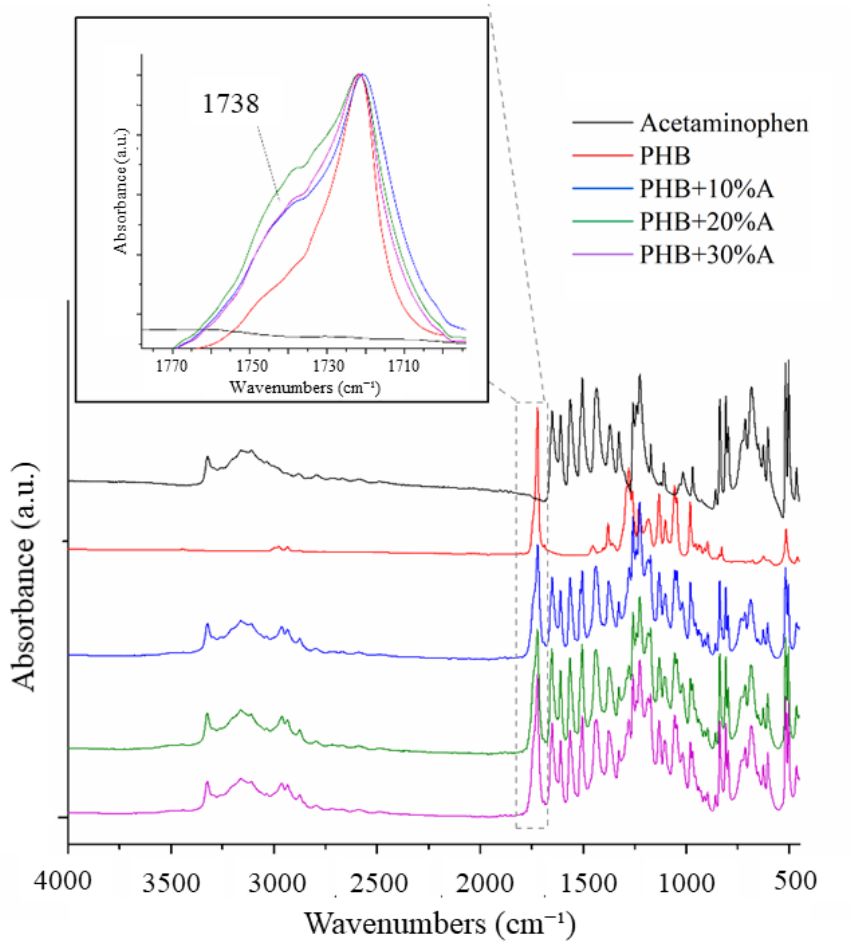

206

207 **Figure 5.** Comparison of the ATR-FTIR spectra of the printed formulations and the starting materials; box: detail of the
208 carbonyl adsorption peak of the PHB.

209 Comparing the spectra of the formulations (PHB+30%A, PHB+20%A, and PHB+10%A) with the starting
210 materials, it is possible to see that the printed devices presented the characteristic peaks of acetaminophen
211 (attribute to the presence of the amide group) and PHB (related to the ester group), suggesting that both
212 materials were successfully incorporated in the final products without affecting their physicochemical
213 characteristics. The detailed description of the typical peaks ranging between 600 and 1600 cm^{-1} of the raw
214 materials has already been described by several researchers (Trivedi et al., 2015) (Ramezani et al., 2015). The
215 shape of PHB bands at 1720 cm^{-1}, related to the carbonyl absorption of the ester groups of the samples with
216 different amounts of acetaminophen was compared (Box of figure 6). Instead, in the range where this band
217 falls there isn't any adsorption of acetaminophen; therefore this band can be used to study the differences in
218 the vibration energies of the PHB C=O groups in the different samples. In order to do that, the PHB C=O bands
219 of the different samples were normalised using the adsorption at 1720 cm^{-1} as reference. As observed,

compared to pure PHB, the samples with acetaminophen showed a more pronounced shoulder at 1738 cm^{-1}, likely due to the presence of less organized PHB crystals where the C=O groups have higher vibration energies due to the lower complexity of the environmental chemical surroundings. In agreement with the DSC analysis, the shoulder is more pronounced in the sample containing the 20% of acetaminophen, thereby being the sample prevalently characterized by the less organized crystallites with the lowest thermal stability.

3.4 Drug release studies

Release studies performed for 21 days in PBS at pH 7.4 are illustrated in figure 6. The release profile of the printed products demonstrated to be dependent on the geometry of the devices, indeed, independently on the formulation, by increasing the size, higher concentrations of acetaminophen were quantified. The effect of the dimensions on release rate can be attributed to the higher surface area that allows greatest water contact and faster release. In addition, increasing the content of the model drug determined higher and accelerated release, indeed, the formulation PHB+30%A, showed a faster dissolution, compared with the other samples. Comprehensively, all devices showed a prolonged release of the model drug.

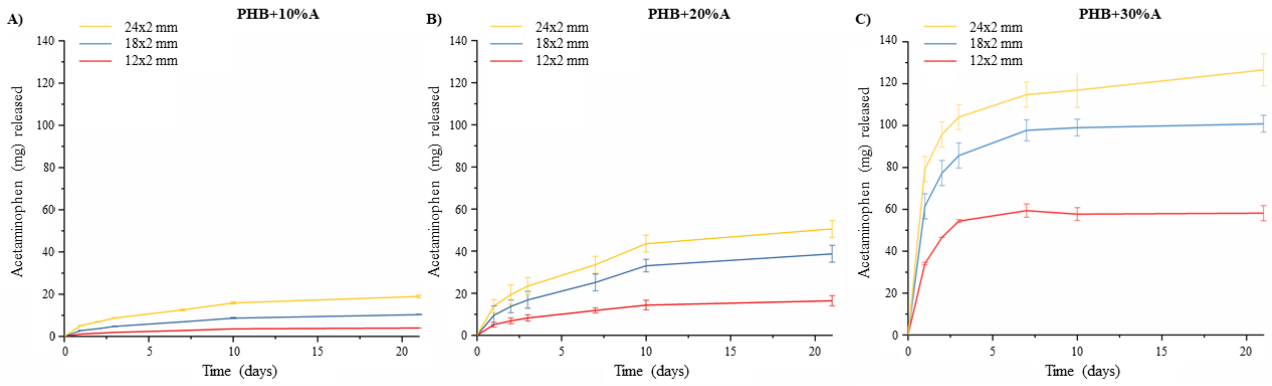

Figure 6. Release profile of A) PHB+10%A, B) PHB+20%A, and C) PHB+30%A.

The release profiles of acetaminophen from the printed formulations were fitted with empirical mathematical models as: the zero order (equation 2), which is based on the exclusive dependency on time; first order (equation 3), based on concentration dependency, and Higuchi (equation 4), which considers the diffusion process dependent on time:

$$Q_t = Q_0 + k_0 t \quad (2)$$

$$Q_t = Q_0 e^{-kt} \quad (3)$$

$$Q_t = k_H t^{1/2} \quad (4)$$

where Q_t is the cumulative drug released at time t, Q_0 is the initial amount of drug release, k_0 (concentration/time) the zero-order kinetic constant, k_1 (time^{-1}) the first-order kinetic constant and k_H (concentration/time$^{1/2}$) the dissolution constant (Malekjani and Jafari, 2021).

Moreover, the semi-empirical Korsemeyer-Peppas model was also considered (equation 5):

$$M_t/M_0 = k_{KP} t^n \quad (5)$$

where M_t/M_0 is the released fraction of drug at at time t, k_{KP} the kinetic constant and n the release exponent indicative of the release mechanism (Malekjani and Jafari, 2021). The kinetic parameters are summarized in table 3.

Table 3. Kinetics parameters of drug release studies.

	MODEL								
	Zero		**First**		**Higuchi**		**Korsemeyer-Peppas**		
Samples	k (g/m^3/h)	R^2	k (1/s)	R^2	k (g/m^3/h$^{0.5}$)	R^2	k (t^{-n})	n	R^2
PHB10% (12x2)	0,004±0,001	0,73539	0,06±0,02	0,67682	0,024±0,002	0,95313	0,034±0,003	0,40±0,04	0,97333
PHB10% (18x2)	0,5±0,1	0,78192	0,06±0,01	0,72537	0,029±0,002	0,9739	0,037±0,003	0,42±0,03	0,98515
PHB10% (24x2)	0,006±0,001	0,77908	0,06±0,01	0,72679	0,030±0,002	0,97355	0,040±0,003	0,41±0,03	0,98615
PHB20% (12x2)	0,009±0,002	0,71555	0,05±0,01	0,68722	0,052±0,005	0,95029	0,080±0,006	0,40±0,03	0,98218
PHB20% (18x2)	0,010±0,002	0,78755	0,06±0,02	0,70737	0,055±0,004	0,97085	0,067±0,006	0,44±0,04	0,9782
PHB20% (24x2)	0,007±0,002	0,76537	0,06±0,01	0,71409	0,041±0,003	0,96653	0,055±0,005	0,41±0,03	0,9814
PHB30% (12x2)	0,01±0,01	0,20558	0,02±0,01	0,20291	0,103±0,035	0,56066	0,38±0,03	0,14±0,04	0,93862
PHB30% (18x2)	0,012±0,007	0,25528	0,018±0,008	0,40578	0,08±0,02	0,60783	0,28±0,01	0,14±0,03	0,97452
PHB30% (24x2)	0,007±0,004	0,28366	0,018±0,007	0,57133	0,05±0,01	0,62758	0,180±0,006	0,14±0,01	0,9909

As can be seen, the acetaminophen is released consistently with the Higuchi model from all the samples except for those containing the 30 % of the drug (R^2 values higher than 0.95) suggesting that the drug release is a diffusion process based on the Fick's law, square root time dependant. Also, the semiempirical Korsemeyer-Peppas model well describe all the drug release profiles of acetaminophen from all the samples (R^2>0.97). Moreover, the n values fall between 0.40-0.45 confirming that the release mechanism is a Fickian diffusion. The samples containing the 30 % are the only exception since they showed a n value of 0.14, significantly below 0.4. A similar value also obtained by Michailidou et al. was attributed to a quasi-Fickian diffusion mechanism of the drug from the polymer network (Michailidou et al., 2019).

In order to understand how the formulation parameters in terms of drug loading and geometry influence the kinetic of the acetaminophen release, in figure 7, the kinetic constants k_{HP} are plotted in function of the dimensions of the square models and of their drug loading. As expected, the drug release occurs faster at lower dimensions and higher loadings. Nevertheless, for drug loading lower than 20 %, any significant contribution in accelerating the drug release does not occur by reducing the dimensions of the design.

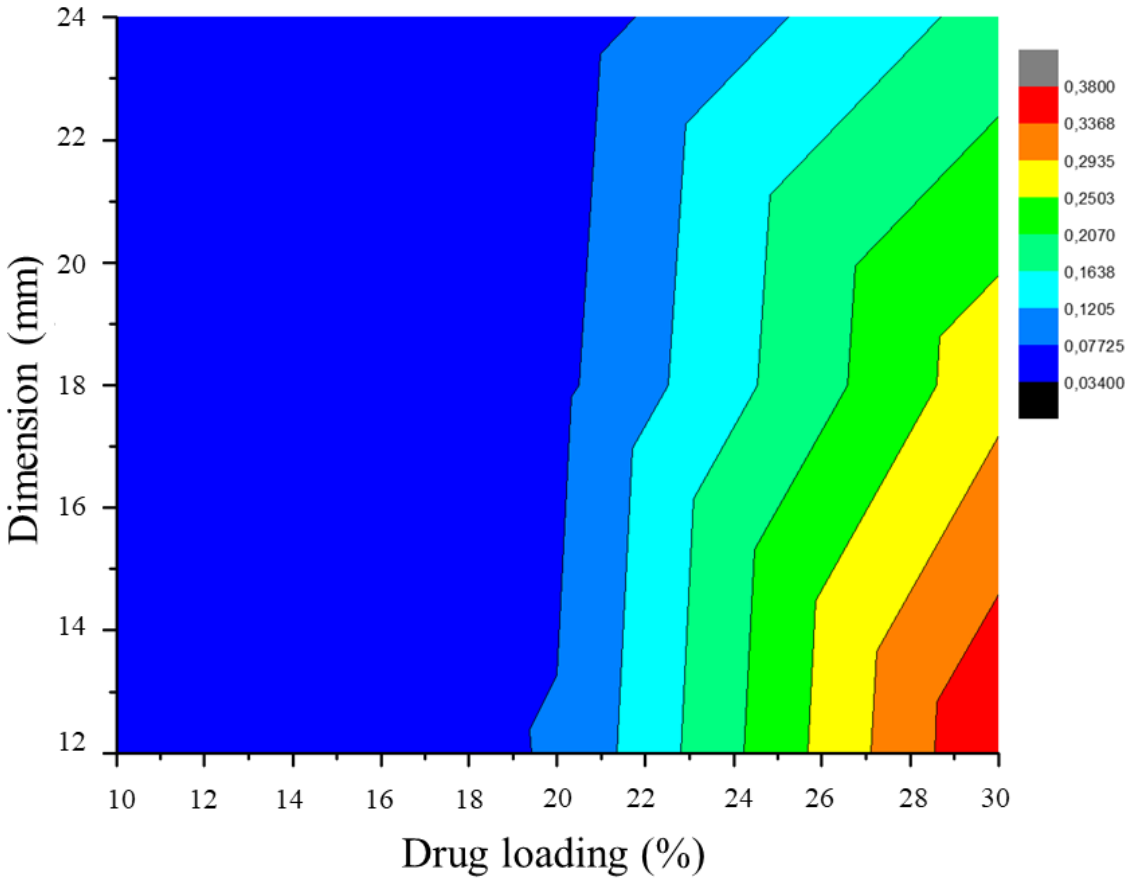

Figure 7. Kinetic constants k_{HP} as a function of tablets dimensions and loadings of acetaminophen.

4. Conclusions

The application of PHB in direct powder extrusion technique has been demonstrated for the first time. Considering the results obtained, we strongly believe that PHB can be an alternative biopolymer for the preparation of prolonged drug release devices. In addition, the direct powder extrusion technique has proven to be a versatile platform in the personalisation of shape and dosage forms, marking another significant step towards the realisation of 3D printed personalised medicine. This approach could be potentially applied in hospitals and pharmacies. However, the technological advancements of 3DP techniques prevail on the availability of materials that are specifically developed for 3DP extrusion and processability. Therefore, the choice of the adequate excipient still remains a challenge to overcame. For this reason, applicative research is necessary to assess material and technique compatibility, thus, improving the performance resolution.

CRediT Autorship

Sofia Moroni: Methodology, Investigation, Formal analysis, Data curation, Writing - original draft.

Shiva Khorshid: Investigation, Data curation.

Annalisa Aluigi: Methodology, Data curation, Writing - review & editing.

Mattia Tiboni: Conceptualization, Supervision, Methodology, Formal analysis, Data curation, Writing - review & editing

Luca Casettari: Conceptualization, Resources, Funding acquisition, Project administration, Supervision, Writing - review & editing.

Funding

Sofia Moroni acknowledge Marche Region for the PhD scholarship (Innovative doctoral programme POR Marche FSE 2014/2020 D.R. 354/2020)

Conflict of interest

The authors declare no conflict of interest

Acknowledgements

297 The authors acknowledge ITIS E. Mattei (Urbino, PU, Italy) for the utilization of FTIR instrument and Fabio
298 De Belvis for the design of the graphical abstract.

299

300 **References**

301 Araújo, M.R.P., Sa-Barreto, L.L., Gratieri, T., Gelfuso, G.M., Cunha-Filho, M., 2019. The digital pharmacies
302 era: How 3D printing technology using fused deposition modeling can become a reality. Pharmaceutics
303 11. https://doi.org/10.3390/pharmaceutics11030128

304 Awad, A., Tren, S.J., Gaisford, S., Basit, A.W., 2018. 3D printed medicines : A new branch of digital
305 healthcare 548, 586–596. https://doi.org/10.1016/j.ijpharm.2018.07.024

306 Boniatti, J., Januskaite, P., da Fonseca, L.B., Viçosa, A.L., Amendoeira, F.C., Tuleu, C., Basit, A.W.,
307 Goyanes, A., Ré, M.I., 2021. Direct powder extrusion 3d printing of praziquantel to overcome
308 neglected disease formulation challenges in paediatric populations. Pharmaceutics 13.
309 https://doi.org/10.3390/pharmaceutics13081114

310 Elmowafy, E., Abdal-Hay, A., Skouras, A., Tiboni, M., Casettari, L., Guarino, V., 2019.
311 Polyhydroxyalkanoate (PHA): Applications in drug delivery and tissue engineering. Expert Rev. Med.
312 Devices 16, 467–482. https://doi.org/10.1080/17434440.2019.1615439

313 Fanous, M., Gold, S., Muller, S., Hirsch, S., Ogorka, J., 2020. Simplification of fused deposition modeling
314 3D-printing paradigm : Feasibility of 1-step direct powder printing for immediate release dosage form
315 production. Int. J. Pharm. 578, 119124. https://doi.org/10.1016/j.ijpharm.2020.119124

316 Giubilini, A., Bondioli, F., Messori, M., Nyström, G., Siqueira, G., 2021. Advantages of Additive
317 Manufacturing for Biomedical Applications of Polyhydroxyalkanoates.

318 Goyanes, A., Allahham, N., Tren, S.J., Stoyanov, E., Gaisford, S., Basit, A.W., 2019. Direct powder
319 extrusion 3D printing : Fabrication of drug products using a novel single-step process 567.
320 https://doi.org/10.1016/j.ijpharm.2019.118471

321 Goyanes, A., Scarpa, M., Kamlow, M., Gaisford, S., Basit, A.W., Orlu, M., 2017. Patient acceptability of 3D
322 printed medicines. Int. J. Pharm. 530, 71–78. https://doi.org/10.1016/j.ijpharm.2017.07.064

323 Gunaratne, L.M.W.K., Shanks, R.A., 2005. Multiple melting behaviour of poly(3-hydroxybutyrate-co-
324 hydroxyvalerate) using step-scan DSC. Eur. Polym. J. 41, 2980–2988.
325 https://doi.org/10.1016/j.eurpolymj.2005.06.015

326 Han, S., Kathuria, H., Jia, J., Tan, Y., Kang, L., 2018. 3D printed drug delivery and testing systems — a
327 passing fad or the future ? Adv. Drug Deliv. Rev. 132, 139–168.
328 https://doi.org/10.1016/j.addr.2018.05.006

329 Koller, M., 2018. Biodegradable and biocompatible polyhydroxy-alkanoates (PHA): Auspicious microbial
330 macromolecules for pharmaceutical and therapeutic applications. Molecules 23.
331 https://doi.org/10.3390/molecules23020362

332 Macedo, J., Samaro, A., Vanhoorne, V., Vervaet, C., Pinto, J.F., 2020. Processability of poly(vinyl alcohol)
333 Based Filaments With Paracetamol Prepared by Hot-Melt Extrusion for Additive Manufacturing. J.
334 Pharm. Sci. 109, 3636–3644. https://doi.org/10.1016/j.xphs.2020.09.016

335 Malekjani, N., Jafari, S.M., 2021. Modeling the release of food bioactive ingredients from
336 carriers/nanocarriers by the empirical, semiempirical, and mechanistic models. Compr. Rev. Food Sci.
337 Food Saf. 20, 3–47. https://doi.org/10.1111/1541-4337.12660

338 Martins, L.S., Cortat, L.I.C.C.O., Zanini, N.C., Barbosa, R.F.S., Souza, A.G., Medeiros, S.F., Rosa, D.S.,
339 Mulinari, D.R., 2021. A versatile filler in polyhydroxyalcanoates filaments for FDM: A diverse
340 panorama for pullulan application. Mater. Today Commun. 28, 102690.
341 https://doi.org/10.1016/j.mtcomm.2021.102690

342 Mathew, E., Pitzanti, G., Larrañeta, E., Lamprou, D.A., 2020. Three-dimensional printing of pharmaceuticals
343 and drug delivery devices. Pharmaceutics 12, 1–9. https://doi.org/10.3390/pharmaceutics12030266

344 Melocchi, A., Uboldi, M., Cerea, M., Foppoli, A., Maroni, A., Moutaharrik, S., Palugan, L., Zema, L.,

345 Gazzaniga, A., 2020. A Graphical Review on the Escalation of Fused Deposition Modeling (FDM) 3D
346 Printing in the Pharmaceutical Field. J. Pharm. Sci. 109, 2943–2957.
347 https://doi.org/10.1016/j.xphs.2020.07.011

348 Michailidou, G., Christodoulou, E., Nanaki, S., Barmpalexis, P., Karavas, E., Vergkizi-Nikolakaki, S.,
349 Bikiaris, D.N., 2019. Super-hydrophilic and high strength polymeric foam dressings of modified
350 chitosan blends for topical wound delivery of chloramphenicol. Carbohydr. Polym. 208, 1–13.
351 https://doi.org/10.1016/j.carbpol.2018.12.050

352 Ngo, T.D., Kashani, A., Imbalzano, G., Nguyen, K.T.Q., Hui, D., 2018. Additive manufacturing (3D
353 printing): A review of materials , methods , applications and challenges. Compos. Part B 143, 172–
354 196. https://doi.org/10.1016/j.compositesb.2018.02.012

355 Ong, J.J., Awad, A., Martorana, A., Gaisford, S., Stoyanov, E., Basit, A.W., Goyanes, A., 2020. 3D printed
356 opioid medicines with alcohol-resistant and abuse-deterrent properties. Int. J. Pharm. 579, 119169.
357 https://doi.org/10.1016/j.ijpharm.2020.119169

358 Ramezani, M., Amoozegar, M.A., Ventosa, A., 2015. Screening and comparative assay of poly-
359 hydroxyalkanoates produced by bacteria isolated from the Gavkhooni Wetland in Iran and evaluation of
360 poly-β-hydroxybutyrate production by halotolerant bacterium Oceanimonas sp. GK1. Ann. Microbiol.
361 65, 517–526. https://doi.org/10.1007/s13213-014-0887-y

362 Seoane-Viaño, I., Trenfield, S.J., Basit, A.W., Goyanes, A., 2021. Translating 3D printed pharmaceuticals:
363 From hype to real-world clinical applications. Adv. Drug Deliv. Rev. 174, 553–575.
364 https://doi.org/10.1016/j.addr.2021.05.003

365 Sinisi, A., Degli Esposti, M., Braccini, S., Chiellini, F., Guzman-Puyol, S., Heredia-Guerrero, J.A., Morselli,
366 D., Fabbri, P., 2021. Levulinic acid-based bioplasticizers: A facile approach to enhance the thermal and
367 mechanical properties of polyhydroxyalkanoates. Mater. Adv. 2, 7869–7880.
368 https://doi.org/10.1039/d1ma00833a

369 Tiboni, M., Campana, R., Frangipani, E., Casettari, L., 2021a. 3D printed clotrimazole intravaginal ring for
370 the treatment of recurrent vaginal candidiasis. Int. J. Pharm. 596, 120290.
371 https://doi.org/10.1016/j.ijpharm.2021.120290

372 Tiboni, Mattia, Tiboni, Massimiliano, Pierro, A., Del Papa, M., Sparaventi, S., Cespi, M., Casettari, L.,
373 2021b. Microfluidics for nanomedicines manufacturing: An affordable and low-cost 3D printing
374 approach. Int. J. Pharm. 599, 120464. https://doi.org/10.1016/j.ijpharm.2021.120464

375 Trenfield, S.J., Goyanes, A., Gaisford, S., Basit, A.W., 2021. Editorial: Innovations in 2D and 3D printed
376 pharmaceuticals. Int. J. Pharm. https://doi.org/10.1016/j.ijpharm.2021.120839

377 Trivedi MK., 2015. Effect of Biofield Treatment on Spectral Properties of Paracetamol and Piroxicam.
378 Chem. Sci. J. 6. https://doi.org/10.4172/2150-3494.100098

379 Wellen, R.M.R., Canedo, E.L., Rabello, M.S., 2015. Melting and crystallization of poly(3-
380 hydroxybutyrate)/carbon black compounds. Effect of heating and cooling cycles on phase transition. J.
381 Mater. Res. 30, 3211–3226. https://doi.org/10.1557/jmr.2015.287

382